

Z-portal Continuum Dark Matter

Csaba Csáki,¹ Sungwoo Hong,^{1, 2, 3} Gowri Kurup,^{1, 4} Seung J. Lee,⁵ Maxim Perelstein,¹ and Wei Xue⁶

¹*Department of Physics, LEPP, Cornell University, Ithaca, NY 14853, USA*

²*Department of Physics, The University of Chicago, Chicago, IL 60637, USA*

³*Argonne National Laboratory, Lemont, IL 60439, USA*

⁴*Department of Physics, University of Oxford, Parks Rd, Oxford OX1 3PJ, United Kingdom*

⁵*Department of Physics, Korea University, Seoul, 136-713, Korea*

⁶*Department of Physics, University of Florida, Gainesville, FL 32611, USA*

We examine the possibility that dark matter (DM) consists of a gapped continuum, rather than ordinary particles. A Weakly-Interacting Continuum (WIC) model, coupled to the Standard Model via a Z-portal, provides an explicit realization of this idea. The thermal DM relic density in this model is naturally consistent with observations, providing a continuum counterpart of the “WIMP miracle”. Direct detection cross sections are strongly suppressed compared to ordinary Z-portal WIMP, thanks to a unique effect of the continuum kinematics. Continuum DM states decay throughout the history of the universe, and observations of cosmic microwave background place constraints on potential late decays. Production of WICs at colliders can provide a striking cascade-decay signature. We show that a simple Z-portal WIC model with the gap scale between 40 and 110 GeV provides a fully viable DM candidate consistent with all current experimental constraints.

INTRODUCTION

Strong evidence from cosmology and astrophysics points to the existence of dark matter (DM), which cannot be made up of standard model (SM) particles. Many viable DM models assuming the existence of some form of new physics have been proposed. Among these, the weakly-interacting massive particle (WIMP) DM [1] has been the leading paradigm for decades. WIMPs naturally arise from well-motivated theoretical extensions of the standard model, such as the neutralino DM in supersymmetry [2]. The WIMP paradigm naturally reproduces the observed DM density; moreover, the relic abundance of WIMPs is insensitive to the initial conditions of the Universe due to the thermal equilibrium between the DM and SM gases in the early Universe. However, experimental searches for non-gravitational signatures of WIMPs have not found any positive evidence yet, leading to increasingly tight constraints on this idea [3]. For example Z-portal DM, one of the simplest and most natural WIMP models, is ruled out by several orders of magnitude [4] by dark matter direct detection experiments [5–7].

In this letter, together with a companion paper [11], we propose a novel framework for DM, based on quantum field theories with a gapped continuum spectrum. Rather than ordinary particles, in such models DM consists of a mixture of states with a continuous mass distribution above a certain “gap” scale μ_0 . Within this framework, we focus on the “weakly-interacting continuum” (WIC) scenario, where the gap $\mu_0 \sim 100$ GeV is near the electroweak scale and the continuum DM interacts with the SM via weak interactions. We will argue that such a WIC model will maintain all the attractive features of WIMPs, including the natural consistency with the observed DM abundance and insensitivity of relic density to

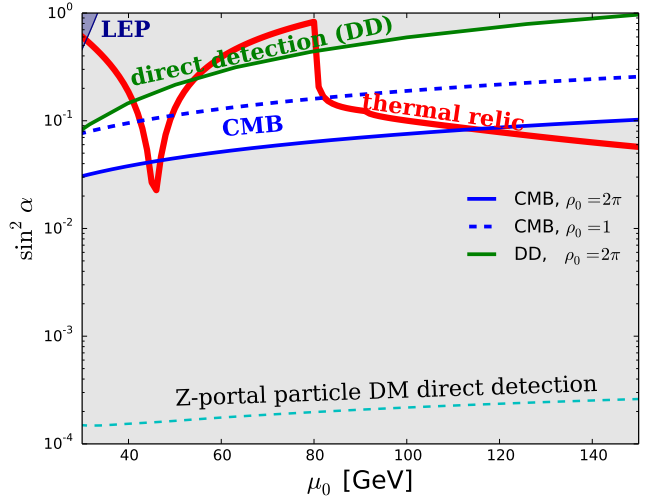


Figure 1: Parameter space of the Z-portal WIC. The red curve corresponds to the thermal relic consistent with observations [8]. The constraints from CMB [9, 10] are shown in the solid (dotted) blue line and region below for $\rho_0 = 2\pi$ ($\rho_0 = 1$). The region consistent with DM direct detection bounds from the XENON1T experiment [5] corresponds to the region below the solid green curve for $\rho_0 = 2\pi$ (no constraints for $\rho_0 = 1$). LEP bound from the invisible Z decay is shown in dark blue region for $\rho_0 = 2\pi$. For comparison, the bound of DM direct detection for Z-portal *particle* DM is shown as the dotted cyan curve.

initial conditions. At the same time the continuum nature of the DM will lead to crucial new phenomenological

features not present in any other DM model.¹ In particular, the distinct kinematics of low-energy scattering of continuum states leads to strong suppression of direct detection rates, reviving the possibility of Z-portal DM. In this paper we will focus on the Z-portal model as a simple and explicit realization of WIC paradigm. The second unique phenomenological feature is that throughout the history of the Universe, DM states continuously decay via $DM(\mu_1) \rightarrow DM(\mu_2) + SM$ processes. Late decays of this sort may leave observational effects in the cosmic microwave background (CMB) due to energy deposition during and after the recombination epoch. There are also interesting effects in collider physics: kinematics of the continuum lead to suppression of DM production rates close to the threshold, weakening some of the collider bounds. On the other hand, production of heavy DM states leads to potentially spectacular signatures as they cascade-decay to invisible states near the gap and SM particles with characteristic multiplicities and spectra.

Gapped continuum theories have been used in various contexts in particle and condensed matter physics, including applications of unparticles [22] to Higgs physics and the hierarchy problem [23–26], string theory [27], the fractional quantum Hall effect [28, 29] or the 2D Ising model [30]. The theoretical framework for quantitative studies of continuum DM was presented in detail in the companion paper [11]. There we described how to construct the Hilbert space of gapped continuum theories, gave formulae for calculating rates of scattering and decay involving continuum DM states, and discussed how to treat their equilibrium and non-equilibrium thermodynamics. We also presented an explicit model of Z-portal WIC, based on a warped 5D soft-wall geometry [31, 32], and applied our formalism to calculate the DM relic density in this model. After giving a brief review of the Z-portal WIC model, this letter focuses on its phenomenology. The main results of our analysis are summarized in fig. 1: it is demonstrated that for mass gap between 40 and 110 GeV, the Z-portal WIC model can reproduce the observed DM density while being fully consistent with current experimental constraints, including direct detection, CMB, and collider data.

Z-PORTAL WIC MODEL

In this section, we briefly review the 4D effective field theory for the Z-portal WIC. Details of the construction, and its realization starting from a local, unitary theory on a 5D soft-wall background, can be found in Ref. [11].

The continuum DM is described by a “generalized free field” Φ , with an effective Lagrangian

$$S = \int \frac{d^4 p}{(2\pi)^4} \Phi^\dagger(p) \Sigma(p^2) \Phi(p). \quad (1)$$

In our model, Φ is a complex, gauge-singlet Lorentz scalar. The spectral density ρ can be obtained as

$$\rho(\mu^2) = -2 \operatorname{Im} \frac{1}{\Sigma(\mu^2)}. \quad (2)$$

In a gapped continuum theory, ρ has continuous support above the gap scale μ_0^2 , and vanishes below that scale. Physically, the continuous parameter μ plays the role of the mass, and we will simply refer to it as the “DM state mass” in this letter. The singly-excited sector of the Hilbert space consists of states $|\mathbf{p}, \mu^2\rangle$, and the spectral density represents the density of states with respect to μ^2 . If the continuum arises from a known 5D theory, the spectral density can be calculated. The behavior of ρ in the vicinity of the gap scale is especially important for DM phenomenology, since during thermal freeze-out and throughout the subsequent evolution of the universe up to our own epoch, most of the DM states are clustered near the gap (see appendix). It was shown in [11] that in a broad range of models, the spectral density near the gap takes the generic form

$$\rho(\mu^2) = \frac{\rho_0}{\mu_0^2} \left(\frac{\mu^2}{\mu_0^2} - 1 \right)^{1/2}, \quad (3)$$

where ρ_0 is a dimensionless constant. The value of ρ_0 is model-dependent, but is typically of order one. In fig. 1 we show constraints for $\rho_0 = 1$ and 2π , but larger or smaller values are also possible.

To couple Φ to the SM sector, a new complex scalar χ is introduced, which is an $SU(2)$ doublet and carries a $U(1)_Y$ charge, $Y = -\frac{1}{2}$. The field χ has a canonical kinetic term and a positive mass-squared m_χ^2 , which we assume to be relatively high, $m_\chi \gg \mu_0$. An interaction term coupling the Higgs H , χ and Φ is allowed by symmetry,

$$\mathcal{L}_{int} = -\lambda \Phi \chi H + \text{h.c.} \quad (4)$$

After electroweak symmetry breaking, the zero-charge component of χ , denoted as χ^0 , mixes with the continuum Φ due to the interactions in eq. (4). Integrating out the χ field yields an effective Lagrangian coupling the continuum to the electroweak gauge bosons:

$$\begin{aligned} \mathcal{L}_{\Phi-Z,W} = \sin^2 \alpha & \left[-\frac{i\sqrt{g^2 + g'^2}}{2} (\partial_\mu \Phi^\dagger \Phi - \Phi^\dagger \partial_\mu \Phi) Z^\mu \right. \\ & \left. + \frac{g^2 + g'^2}{4} \Phi^\dagger \Phi Z_\mu Z^\mu + \frac{1}{2} g^2 \Phi^\dagger \Phi W_\mu^+ W^{-\mu} \right]. \quad (5) \end{aligned}$$

¹ Our model shares some features with dynamical DM models proposed in [12–21], but the two frameworks also have important differences in both model-building and phenomenological predictions. For a more detailed comparison, see Ref. [11].

Here g and g' are the SM $SU(2)_L$ and $U(1)_Y$ gauge couplings, and the mixing angle α is given by

$$\tan 2\alpha = \frac{\sqrt{2} \lambda v}{m_\chi^2 - \mu^2}. \quad (6)$$

These are the interactions responsible for WIC annihilation and decay to the SM particles. Note that the interactions preserve the total number of the DM continuum states, due to a Z_2 parity, even though they allow such states to decay into each other. The physics of WIC is described in terms of just three new parameters (the gap scale μ_0 , the mixing angle α , and the spectral density normalization ρ_0), making for a simple and predictive model.

BOLTZMANN EQUATIONS AND THERMAL RELIC

A dilute gas of continuum DM states is described by the occupation number $f(\mathbf{p}, \mu)$. In thermal equilibrium, the occupation number follows the usual Fermi-Dirac or Bose-Einstein distribution, with particle mass m replaced by the continuum state mass μ . The number density of continuum states is given by

$$n = \int \frac{d\mu^2}{2\pi} \nu(\mu^2), \quad (7)$$

where

$$\nu(\mu^2) = \rho(\mu^2) \int \frac{d^3 p}{(2\pi)^3} f(\mathbf{p}, \mu) \quad (8)$$

is the DM mass distribution function. When considering the continuum annihilation to the SM particles during the freeze-out process, the Boltzmann equation for the continuum has the usual form (see detailed derivation in [11]),

$$\frac{\partial n}{\partial t} + 3H n = -\langle \sigma v \rangle (n^2 - n_{\text{eq}}^2), \quad (9)$$

where n_{eq} is the number density in thermal equilibrium. The thermal relic density for WIC is the same as for WIMP with the same thermally-averaged cross section $\langle \sigma v \rangle$, but for WIC $\langle \sigma v \rangle$ includes averaging over μ^2 . In practice, taking into account the Boltzmann factor and the form of the spectral density near the gap, eq. (3), it is easy to see that the continuum distribution at temperatures below μ_0 is localized near the gap scale. The WIC relic density is then the same as for a WIMP of mass $m = \mu_0$ and interactions in eq. (5), up to small corrections of order $\mathcal{O}(T^2/\mu^2)$. Note that the thermal relic density does not depend on ρ_0 , since the normalization of the spectral density cancels out in the $\langle \sigma v \rangle$.

The dominant WIC annihilation process during freeze-out depends on the gap scale μ_0 . In the regime of

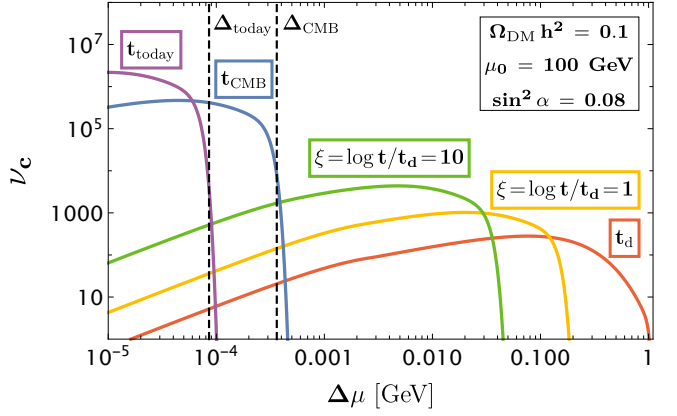


Figure 2: Time evolution of the DM comoving number density ν_c , as a function of mass above the gap $\Delta\mu = \mu - \mu_0$, after its kinetic decoupling from the SM at time t_d . The black lines indicate Δ_{CMB} and Δ_{today} , found analytically by setting $\Gamma = H$ at photon decoupling and today, respectively. The y-axis units are arbitrary. See appendix for details.

$\mu_0 < m_W$, the dominant channel is $\Phi\Phi^* \rightarrow Z \rightarrow f\bar{f}$. This process is p-wave, since the parity of the initial state is -1 . For a larger gap scale, $\mu_0 \gtrsim m_{W,Z}$, s-wave annihilations into pairs of vector bosons becomes relevant, $\Phi\Phi^* \rightarrow W^+W^-$ and $\Phi\Phi^* \rightarrow ZZ$. In fig. 1, the red curve corresponds to the observed DM relic abundance. The required value of the mixing angle $\sin^2 \alpha$ drops near the Z-pole, $\mu_0 \simeq m_Z/2$, where the cross section is enhanced by the Z-pole resonance. The decrease of the required $\sin^2 \alpha$ above m_W is due to the fact that more annihilation channels are open. Note that we do not include the WIC annihilations to one on-shell and one off-shell W, which may give order-one corrections to the total annihilation rate in a narrow region of μ_0 just below m_W .

LATE DECAY AND CMB CONSTRAINTS

One of the main distinguishing features of WIC DM compared to ordinary particle DM is that throughout the history of the universe, the continuum states are continuously decaying to the SM particles, $\Phi(\mu_1) \rightarrow \Phi(\mu_2) + \text{SM}$. These processes are always unavoidable even in the presence of an exact Z_2 symmetry, due to the off-diagonal couplings among the continuum states such as in the interactions in eq. (5). These decays keep dumping energy into the SM sector with $E \simeq \mu_1 - \mu_2$, and can leave imprints during and after the recombination epoch.

The evolution history of the continuum states can be summarized as follows. Before the freeze-out they are in thermal and chemical equilibrium. After the WIC freeze-out, which occurs at $T \sim \mu_0/10$, the quasi-elastic scattering $\Phi + \text{SM} \leftrightarrow \Phi + \text{SM}$ and (inverse) decays $\Phi \leftrightarrow \Phi + \text{SM}$ maintain kinetic equilibrium of the continuum with the

SM particles and chemical equilibrium among the continuum states themselves. This equilibrium will force the mass distribution of the continuum states to peak ever closer to the gap scale μ_0 as the temperature of the SM plasma decreases. At temperature T , a typical DM state has mass μ such that $\Delta\mu \equiv \mu - \mu_0 \sim T$. Eventually, the rate of these processes falls below the Hubble rate, the WICs fully decouple from the SM, and the chemical equilibrium among the continuum states can no longer be maintained. For typical parameters in the Z-portal WIC model, this decoupling occurs at $T_d \sim 0.1 - 1$ GeV. After decoupling, the WIC mass distribution continues to evolve due to out-of-equilibrium WIC decays $\Phi \rightarrow \Phi + \text{SM}$, with typical masses tending ever closer to the gap scale. This evolution is illustrated in fig. 2, which is based on a numerical solution of the Boltzmann equation for a Z-portal WIC model that satisfies the relic density, CMB and direct detection constraints (see appendix). An upper bound on the DM mass μ at any given time t in this epoch can be estimated by equating the total decay rate of $\Phi(\mu)$ with the Hubble rate $H(t)$, since heavier DM states would have already decayed. This estimate agrees well with the numerical results, see fig. 2. A typical DM mass at any given time is within a factor of a few from this bound, which implies that each DM state on average undergoes $\mathcal{O}(1)$ decays per Hubble time.

In the Z-portal WIC model, the DM states decay through an off-shell Z, $\Phi(\mu_1) \rightarrow \Phi(\mu_2) + Z^* \rightarrow \Phi(\mu_2) + f\bar{f}$. The rate of this decay (integrated over μ_2) is given by

$$\Gamma(\Phi \rightarrow \Phi + f\bar{f}) = \frac{16\sqrt{2}\rho_0}{15 \times 9009\pi^4} \sin^4 \alpha \frac{(g^2 + g'^2)^2}{m_Z^4} \times (g_A^2 + g_V^2) (\Delta\mu)^5 \left(\frac{\Delta\mu}{\mu_0} \right)^{3/2} \equiv \Gamma_0 \left(\frac{\Delta\mu}{\mu_0} \right)^{13/2}, \quad (10)$$

where $\Delta\mu = \mu_1 - \mu_0$, and $g_{A,V}$ are the SM Z couplings. The strong dependence on the DM mass arises from three-body phase space $\propto (\Delta\mu)^3$, the matrix element-squared $\propto (\Delta\mu)^2$, and final state spectral density integration $\propto (\Delta\mu/\mu_0)^{3/2}$. Here we assumed $\Delta\mu \gg m_f$; the rate rapidly drops to zero near the kinematic threshold $\Delta\mu = 2m_f$.

For typical WIC parameters, $\Delta\mu$ drops below muon and pion thresholds soon after kinetic decoupling, while the decays to e^+e^- and the three neutrino flavors continue at late times. The first of these decays is potentially problematic for phenomenology, since it injects EM energy which can reionize hydrogen atoms after recombination. For example, if $\Delta\mu = 2$ MeV soon after recombination, electrons of typical kinetic energy \sim MeV would be produced, each of which can reionize $\sim 10^5$ H atoms. Given that $\rho_{\text{DM}}/\rho_H \approx 5$ and that each DM state undergoes $\mathcal{O}(1)$ decays per Hubble time as explained above, the hydrogen would be quickly completely

reionized, in gross conflict with CMB observations. Even decays close to kinematic threshold are ruled out. To avoid this constraint, we require that decays into e^+e^- pairs become kinematically impossible at or before the CMB decoupling time t_{CMB} . We conservatively estimate $\Delta\mu_{\text{CMB}}$ using $\Gamma = H(t_{\text{CMB}})$ (where Γ is the total DM decay rate including neutrino final states), and require $\Delta\mu_{\text{CMB}} < 2m_e \approx 1$ MeV. This constraint gives a *lower* bound on the mixing angle $\sin \alpha$, shown by the blue curves in fig. 1.

In the epoch after recombination, DM states continue to decay via the neutrino channel. As a result of these decays, $\Delta\mu$ decreases by roughly a factor of 3 between the CMB decoupling and today, as can be seen in fig. 2. Neutrinos from such decays could in principle be detected by XENON1T [33], SuperKamiokande [34] and other experiments [35, 36]. However, the predicted neutrino flux from WIC decays is several orders of magnitude smaller than the solar neutrino flux. Therefore, there are currently no constraints on late decays to neutrinos. In the future, these decays may lead to a new window for discovering the Z-portal WIC.

DIRECT DETECTION

Direct detection signature of WIC is due to a scattering process $\text{DM}(\mu) + N \rightarrow \text{DM}(\mu') + N$, where N is a target nucleus. Since μ and μ' are continuous variables, the kinematics of this process in the WIC model is quite distinct from either elastic or inelastic particle DM. This unique kinematics leads to a strong suppression of the direct detection rate, which is one of the most striking features of such models, and allows for a viable Z-portal WIC model consistent with current bounds.

The direct detection rate for the continuum DM is given by

$$\frac{dR}{dE_R} = N_T \int \frac{d\mu^2}{2\pi} \nu_0(\mu^2) \int d^3v f(v) \frac{d\sigma}{dE_R} v \quad (11)$$

where E_R is the recoil energy of the nucleus, N_T the number of nuclei per unit mass, ν_0 is the WIC mass distribution function in the Earth's neighborhood, and $f(v)$ is the local dark matter velocity distribution. We will use the approximation

$$\nu_0 = \frac{\rho_\odot}{\mu_0} \delta(\mu^2 - \mu_1^2), \quad (12)$$

where $\rho_\odot = 0.3$ GeV/cm³ is the local dark matter density, and μ_1 is found by equating the WIC decay rate with today's Hubble scale. (For typical parameters, $\mu_1 - \mu_0 \sim 100 - 300$ keV.) We assume the Maxwell-Boltzmann distribution for the WIC DM with a cutoff at the escape velocity $v_{\text{esc}} = 600$ km/s. Since the DM state masses in today's universe are clustered near the

gap scale with a small relative spread, the velocity distribution is approximately mass-independent. The differential cross section is given by

$$\frac{d\sigma}{dE_R} = \int_{\mu_0^2}^{\mu_{\max}^2} \frac{d\mu'^2}{2\pi} \rho(\mu'^2) \frac{m_N \sigma_p}{2\mu_{\Phi n}^2 v^2} \left[\frac{f_p Z + f_n(A - Z)}{f_p} \right]^2 F_N^2(q). \quad (13)$$

The DM-proton (or neutron) cross section is

$$\sigma_p = \frac{(g^2 + g'^2)^2 \sin^4 \alpha \mu_{\Phi n}^2 f_p^2}{16\pi m_Z^4}. \quad (14)$$

Here $\mu_{\Phi n}$ is the reduced mass of the DM state and proton or neutron, and $F_N(q)$ is the nucleus form factor. (We are using the Helm form factor [37] in this work.) The coupling strength to nucleon f_p (f_n) is given by the vector current matching from the quark to nucleon, $f_n = b_u + 2b_d = -\frac{1}{4}$ and $f_p = 2b_u + b_d = \frac{1}{4} - \sin^2 \theta_w$. The incoming DM state with mass μ_1 can be down-scattered or up-scattered. Using energy-momentum conservation, the maximum accessible mass for the outgoing state is given by

$$\mu_{\max} = \mu_1 + qv - \frac{1}{2} \frac{q^2}{\mu_{\Phi N}}, \quad (15)$$

where $q = \sqrt{2m_N E_R}$ is the exchanged momentum. Since $\mu_1 - \mu_0 \ll \mu_0$ and $v \ll 1$, only a narrow range of DM states are kinematically accessible. In addition the spectral density is small near the gap. Both effects suppress the cross section (13): for typical values,

$$\int_{\mu_0^2}^{\mu_{\max}^2} \frac{d\mu'^2}{2\pi} \rho(\mu'^2) \sim \left(\frac{\Delta\mu}{\mu_0} \right)^{3/2}, \quad (16)$$

which is roughly $\sim \mathcal{O}(10^{-6} - 10^{-7})$.

The Z-portal WIC DM limits from direct detection are obtained by comparing the predicted number of events in this model with the particle DM prediction and recasting the bounds from the XENON1T experiment [5]. (The effect of the continuum kinematics on the nuclear recoil energy spectrum is not large enough to significantly affect the bounds, but may become an important potential discriminator between WIC and particle DM if a signal is observed.) The direct detection bounds are shown in fig. 1 by the green curve for $\rho_0 = 2\pi$. For $\rho_0 = 1$ the kinematic suppression is even larger and there is no constraint. For comparison, the much stronger Z-portal particle DM limits are shown by the dotted cyan curve.

OTHER CONSTRAINTS

The kinematics and the cross section of DM annihilation in today's halos in the WIC model is virtually identical to that of a usual particle DM of mass μ_0 . Therefore,

the standard particle DM analysis for indirect detection can be applied to continuum DM. For Z-portal DM with $\mu_0 < m_W$, the dominant channel is $\Phi\Phi^* \rightarrow Z^* \rightarrow f\bar{f}$, and the rate is p-wave suppressed. For $\mu_0 > m_W$, DM can annihilate via s-wave into WW and ZZ , which can be constrained by the dwarf galaxy data from Fermi-LAT [38]. As is known, the indirect detection bounds suffer from significant uncertainties due to DM distribution and astrophysical backgrounds. After profiling the J-factor distributions and the background uncertainties, thermal-relic s-wave DM is allowed for masses above 30 GeV; see *e.g.* fig. 5 in [39]. (While the bound shown is for annihilation to $b\bar{b}$, the photon spectrum from WW or ZZ final states is very similar.) We conclude that the Z-portal WIC DM is easily consistent with the indirect detection experiments.

At colliders, continuous DM states can be pair-produced in $q\bar{q}$ or e^+e^- annihilation through virtual Z exchange. Each of the produced DM states decays to a lighter DM state plus SM particles (a Z , if kinematically allowed, or quark-lepton pairs, if not). The lighter DM states in turn undergo further decays, until the DM cascades down to a state so close to the gap that its decays are effectively invisible in the detector due to its long lifetime and/or softness of its SM decay products. Overall, the event looks similar to the $X+MET$ signature of neutralino $\tilde{\chi}_2^0$ production in SUSY models, but with higher multiplicity and somewhat softer spectrum of visible particles. In the mass range of interest, SM W pair-production produces the dominant background for this search. Continuum DM production cross sections are suppressed by a factor of $\sin^4 \alpha \sim 10^{-2}$ compared to SM electroweak processes, in addition to continuum kinematic suppression near the mass threshold similar to the suppression of direct detection rates. As a result, the Z-portal DM model is consistent with current LHC bounds. For $\mu_0 < m_Z/2$, where Z -decays to on-shell DM pairs are allowed, strong bounds from LEP-1 and SLD become relevant. However, the bounds on WIC are again much weaker compared to the particle Z-portal DM, due to the continuum kinematic suppression of the decay rate. We conservatively estimate the bound by comparing the rate to the experimental limit on the invisible Z decays Γ_{inv} [40]. The resulting bound is quite weak, see fig. 1. We will explore collider phenomenology of the Z-portal WIC model in detail in future work.

CONCLUSIONS

In this letter we initiated the study of phenomenology of the Z-portal Weakly Interacting Continuum (WIC) model introduced in the companion paper [11]. In this model the role of DM is played by a gapped continuum, rather than an ordinary particle, which acquires couplings to the SM W/Z bosons from mixing induced

via the Higgs. Since at late times (when the temperature is below the gap scale μ_0) the WIC mass distribution is strongly peaked around μ_0 , the thermal freeze-out of WICs is essentially identical to that of ordinary particle WIMPs. However other properties of the WIC are strikingly different. Due to the unique features of continuum kinematics, the direct detection cross section is strongly suppressed, re-opening the Z-portal for WICs. WIC decays of the sort $\Phi(\mu_1) \rightarrow \Phi(\mu_2) + \text{SM}$ occur throughout the history of the universe, with each DM state decaying on average once per Hubble time. Such decays may yield dangerous new sources of e^+e^- pairs during and after the epoch of recombination, resulting in a *lower* bound on the WIC coupling to the SM. The same type of decays will ensure that the generic collider signals of WICs will include a cascade of SM particles (in addition to the invisible final WIC state close to the gap at the end of the cascade). We have shown that the current collider bounds from the LHC and LEP do not significantly constrain the Z-portal WIC model, and neither do the indirect detection or neutrino experiments. We conclude that the Z-portal WIC with a gap scale in the range of about 40-110 GeV provides a fully viable DM candidate consistent with all experimental constraints, as shown in the summary plot in fig. 1. We look forward to further studies of the rich and novel phenomenology of these models.

We are grateful to Francesca Calore, Barry McCoy, Eun-Gook Moon, Carlos Wagner, Liantao Wang and Kathryn Zurek for useful discussions. C.C., S.H. G.K. and M.P. were supported in part by the NSF grant PHY-2014071. C.C. was also supported in part by the US-Israeli BSF grant 2016153. S.H. was also supported by the DOE grants DE-SC-0013642 and DE-AC02-06CH11357 as well as a Hans Bethe Post-doctoral fellowship at Cornell. G.K. is supported by the Science and Technology Facilities Council with Grant No. ST/T000864/1. S.L. was supported by the Samsung Science and Technology Foundation under Project Number SSTF-BA1601-07 and also by the National Research Foundation of Korea (NRF) grant funded by the Korea government (MEST) (No. NRF-2021R1A2C1005615). W.X. was supported in part by the DOE grant DE-SC0010296.

Out-of-Equilibrium Decays

The mass distribution of continuum dark matter states after chemical decoupling follows a Boltzmann equation

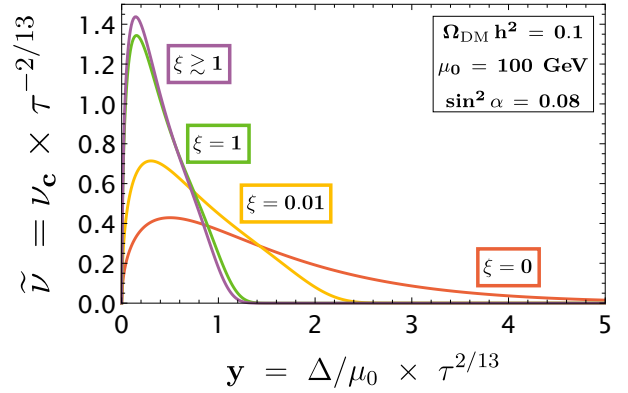


Figure 3: Evolution of mass distribution of DM states in rescaled variables y and ξ . The Z-portal WIC model parameters are such that the relic density, CMB and direct detection constraints are satisfied.

given by

$$\begin{aligned} \frac{\partial \nu(\mu^2)}{\partial t} + 3H\nu(\mu^2) &= -\Gamma(\mu^2)\nu(\mu^2) \\ &+ \int_{\mu^2}^{\infty} d\mu'^2 \nu(\mu'^2) \frac{d\Gamma}{d\mu^2}(\mu'^2 \rightarrow \mu^2) \end{aligned} \quad (17)$$

where the decay rate $\Gamma(\mu^2)$ is given in eq. (10), and

$$\frac{d\Gamma}{d\mu^2}(\mu'^2 \rightarrow \mu^2) = \frac{9009}{1024} \frac{\Gamma_0}{\mu_0^2} \left(\frac{\mu}{\mu_0} - 1 \right)^{1/2} (\mu' - \mu)^5. \quad (18)$$

The first term on the right-hand side of eq. (17) describes the depletion of states with mass μ due to their decays, while the second term represents their re-population due to decays of heavier modes. Note that

$$\Gamma(\mu'^2) = \int_{\mu_0^2}^{\mu'^2} d\mu^2 \frac{d\Gamma}{d\mu^2}(\mu'^2 \rightarrow \mu^2). \quad (19)$$

Using this relation, it is easy to check that the evolution described by eq. (17) conserves the total number of DM states, as expected due to Z_2 symmetry.

The Boltzmann equation can be solved numerically to find the distribution of DM states at each redshift z . The numerical integration is smoother and more stable when μ and t are rescaled as follows: $y = (\mu/\mu_0 - 1) \tau^{2/13}$ and $\xi = \log(t/t_d)$, where $\tau = \Gamma_0 t$ and t_d is the time at decoupling. (This rescaling is suggested by the estimate of the maximum DM mass using $\Gamma = H$, as described in the main text.) Additionally, we rescale the distribution ν as $\tilde{\nu} = \nu_c \tau^{-2/13}$, where $\nu_c(\mu^2) = \nu a^3$ (a = scale factor) is the comoving number density at each mass μ^2 . In the radiation dominated era, $a \propto t^{1/2}$ and $\nu_c = \nu (t/t_d)^{3/2}$. Ignoring overall normalization constants, an example of the evolution of this distribution is shown in fig. 3. The

rescaled mass parameter remains of order one throughout the evolution. The initial evolution is fast, but the distribution stabilizes for $\xi \gtrsim 1$ as shown, and remains essentially the same for $\xi \gg 1$. Rescaling back to the original coordinates produces the distributions shown in fig. 2.

[1] B. W. Lee and S. Weinberg, “Cosmological Lower Bound on Heavy Neutrino Masses,” *Phys. Rev. Lett.* **39** (1977) 165–168.

[2] G. Jungman, M. Kamionkowski, and K. Griest, “Supersymmetric dark matter,” *Phys. Rept.* **267** (1996) 195–373, [arXiv:hep-ph/9506380](https://arxiv.org/abs/hep-ph/9506380).

[3] G. Bertone, D. Hooper, and J. Silk, “Particle dark matter: Evidence, candidates and constraints,” *Phys. Rept.* **405** (2005) 279–390, [arXiv:hep-ph/0404175](https://arxiv.org/abs/hep-ph/0404175).

[4] M. Escudero, A. Berlin, D. Hooper, and M.-X. Lin, “Toward (Finally!) Ruling Out Z and Higgs Mediated Dark Matter Models,” *JCAP* **12** (2016) 029, [arXiv:1609.09079](https://arxiv.org/abs/1609.09079) [hep-ph].

[5] **XENON** Collaboration, E. Aprile *et al.*, “Dark Matter Search Results from a One Ton-Year Exposure of XENON1T,” *Phys. Rev. Lett.* **121** no. 11, (2018) 111302, [arXiv:1805.12562](https://arxiv.org/abs/1805.12562) [astro-ph.CO].

[6] **LUX** Collaboration, D. S. Akerib *et al.*, “Results from a search for dark matter in the complete LUX exposure,” *Phys. Rev. Lett.* **118** no. 2, (2017) 021303, [arXiv:1608.07648](https://arxiv.org/abs/1608.07648) [astro-ph.CO].

[7] **PandaX-II** Collaboration, X. Cui *et al.*, “Dark Matter Results From 54-Ton-Day Exposure of PandaX-II Experiment,” *Phys. Rev. Lett.* **119** no. 18, (2017) 181302, [arXiv:1708.06917](https://arxiv.org/abs/1708.06917) [astro-ph.CO].

[8] **Planck** Collaboration, P. A. R. Ade *et al.*, “Planck 2015 results. XIII. Cosmological parameters,” *Astron. Astrophys.* **594** (2016) A13, [arXiv:1502.01589](https://arxiv.org/abs/1502.01589) [astro-ph.CO].

[9] T. R. Slatyer and C.-L. Wu, “General Constraints on Dark Matter Decay from the Cosmic Microwave Background,” *Phys. Rev. D* **95** no. 2, (2017) 023010, [arXiv:1610.06933](https://arxiv.org/abs/1610.06933) [astro-ph.CO].

[10] T. R. Slatyer, “Indirect dark matter signatures in the cosmic dark ages. I. Generalizing the bound on s-wave dark matter annihilation from Planck results,” *Phys. Rev. D* **93** no. 2, (2016) 023527, [arXiv:1506.03811](https://arxiv.org/abs/1506.03811) [hep-ph].

[11] C. Csáki, S. Hong, G. Kurup, S. J. Lee, M. Perelstein, and W. Xue, “Continuum Dark Matter,” [arXiv:2105.07035](https://arxiv.org/abs/2105.07035) [hep-ph].

[12] K. R. Dienes and B. Thomas, “Dynamical Dark Matter: I. Theoretical Overview,” *Phys. Rev. D* **85** (2012) 083523, [arXiv:1106.4546](https://arxiv.org/abs/1106.4546) [hep-ph].

[13] K. R. Dienes and B. Thomas, “Dynamical Dark Matter: II. An Explicit Model,” *Phys. Rev. D* **85** (2012) 083524, [arXiv:1107.0721](https://arxiv.org/abs/1107.0721) [hep-ph].

[14] K. R. Dienes, S. Su, and B. Thomas, “Distinguishing Dynamical Dark Matter at the LHC,” *Phys. Rev. D* **86** (2012) 054008, [arXiv:1204.4183](https://arxiv.org/abs/1204.4183) [hep-ph].

[15] K. R. Dienes, J. Kumar, and B. Thomas, “Direct Detection of Dynamical Dark Matter,” *Phys. Rev. D* **86** (2012) 055016, [arXiv:1208.0336](https://arxiv.org/abs/1208.0336) [hep-ph].

[16] K. R. Dienes, J. Kumar, B. Thomas, and D. Yaelali, “Overcoming Velocity Suppression in Dark-Matter Direct-Detection Experiments,” *Phys. Rev. D* **90** no. 1, (2014) 015012, [arXiv:1312.7772](https://arxiv.org/abs/1312.7772) [hep-ph].

[17] K. R. Dienes, J. Kumar, B. Thomas, and D. Yaelali, “Dark-Matter Decay as a Complementary Probe of Multicomponent Dark Sectors,” *Phys. Rev. Lett.* **114** no. 5, (2015) 051301, [arXiv:1406.4868](https://arxiv.org/abs/1406.4868) [hep-ph].

[18] K. R. Dienes, S. Su, and B. Thomas, “Strategies for probing nonminimal dark sectors at colliders: The interplay between cuts and kinematic distributions,” *Phys. Rev. D* **91** no. 5, (2015) 054002, [arXiv:1407.2606](https://arxiv.org/abs/1407.2606) [hep-ph].

[19] K. K. Boddy, K. R. Dienes, D. Kim, J. Kumar, J.-C. Park, and B. Thomas, “Lines and Boxes: Unmasking Dynamical Dark Matter through Correlations in the MeV Gamma-Ray Spectrum,” *Phys. Rev. D* **94** no. 9, (2016) 095027, [arXiv:1606.07440](https://arxiv.org/abs/1606.07440) [hep-ph].

[20] D. Curtin, K. R. Dienes, and B. Thomas, “Dynamical Dark Matter, MATHUSLA, and the Lifetime Frontier,” *Phys. Rev. D* **98** no. 11, (2018) 115005, [arXiv:1809.11021](https://arxiv.org/abs/1809.11021) [hep-ph].

[21] K. R. Dienes, D. Kim, H. Song, S. Su, B. Thomas, and D. Yaelali, “Nonminimal dark sectors: Mediator-induced decay chains and multijet collider signatures,” *Phys. Rev. D* **101** no. 7, (2020) 075024, [arXiv:1910.01129](https://arxiv.org/abs/1910.01129) [hep-ph].

[22] H. Georgi, “Unparticle physics,” *Phys. Rev. Lett.* **98** (2007) 221601, [arXiv:hep-ph/0703260](https://arxiv.org/abs/hep-ph/0703260).

[23] D. Stancato and J. Terning, “The Unhiggs,” *JHEP* **11** (2009) 101, [arXiv:0807.3961](https://arxiv.org/abs/0807.3961) [hep-ph].

[24] A. Falkowski and M. Perez-Victoria, “Holographic Unhiggs,” *Phys. Rev. D* **79** (2009) 035005, [arXiv:0810.4940](https://arxiv.org/abs/0810.4940) [hep-ph].

[25] B. Bellazzini, C. Csáki, J. Hubisz, S. J. Lee, J. Serra, and J. Terning, “Quantum Critical Higgs,” *Phys. Rev. X* **6** no. 4, (2016) 041050, [arXiv:1511.08218](https://arxiv.org/abs/1511.08218) [hep-ph].

[26] C. Csáki, G. Lee, S. J. Lee, S. Lombardo, and O. Telem, “Continuum Naturalness,” *JHEP* **03** (2019) 142, [arXiv:1811.06019](https://arxiv.org/abs/1811.06019) [hep-ph].

[27] S. S. Gubser, “Curvature singularities: The Good, the bad, and the naked,” *Adv. Theor. Math. Phys.* **4** (2000) 679–745, [arXiv:hep-th/0002160](https://arxiv.org/abs/hep-th/0002160).

[28] S. Sachdev, “Quantum phase transitions,” *Handbook of Magnetism and Advanced Magnetic Materials* (2007) .

[29] E. H. Fradkin, *Field Theories of Condensed Matter Physics*, vol. 82. Cambridge Univ. Press, Cambridge, UK, 2, 2013.

[30] B. M. McCoy and T. T. Wu, “Two-dimensional Ising Field Theory in a Magnetic Field: Breakup of the Cut in the Two Point Function,” *Phys. Rev. D* **18** (1978) 1259.

[31] L. Randall and R. Sundrum, “A Large mass hierarchy from a small extra dimension,” *Phys. Rev. Lett.* **83** (1999) 3370–3373, [arXiv:hep-ph/9905221](https://arxiv.org/abs/hep-ph/9905221).

[32] J. A. Cabrer, G. von Gersdorff, and M. Quiros, “Soft-Wall Stabilization,” *New J. Phys.* **12** (2010) 075012, [arXiv:0907.5361](https://arxiv.org/abs/0907.5361) [hep-ph].

[33] **XENON** Collaboration, E. Aprile *et al.*, “Excess electronic recoil events in XENON1T,” *Phys. Rev. D* **102** no. 7, (2020) 072004, [arXiv:2006.09721](https://arxiv.org/abs/2006.09721) [hep-ex].

[34] **Super-Kamiokande** Collaboration, K. Bays *et al.*, “Supernova Relic Neutrino Search at Super-Kamiokande,” *Phys. Rev. D* **85** (2012) 052007,

arXiv:1111.5031 [hep-ex].

[35] **BOREXINO** Collaboration, M. Agostini *et al.*, “Sensitivity to neutrinos from the solar CNO cycle in Borexino,” *Eur. Phys. J. C* **80** no. 11, (2020) 1091, arXiv:2005.12829 [hep-ex].

[36] **BOREXINO** Collaboration, M. Agostini *et al.*, “Experimental evidence of neutrinos produced in the CNO fusion cycle in the Sun,” *Nature* **587** (2020) 577–582, arXiv:2006.15115 [hep-ex].

[37] J. D. Lewin and P. F. Smith, “Review of mathematics, numerical factors, and corrections for dark matter experiments based on elastic nuclear recoil,” *Astropart. Phys.* **6** (1996) 87–112.

[38] **Fermi-LAT, DES** Collaboration, A. Albert *et al.*, “Searching for Dark Matter Annihilation in Recently Discovered Milky Way Satellites with Fermi-LAT,” *Astrophys. J.* **834** no. 2, (2017) 110, arXiv:1611.03184 [astro-ph.HE].

[39] A. Alvarez, F. Calore, A. Genina, J. Read, P. D. Serpico, and B. Zaldivar, “Dark matter constraints from dwarf galaxies with data-driven J-factors,” *JCAP* **09** (2020) 004, arXiv:2002.01229 [astro-ph.HE].

[40] **Particle Data Group** Collaboration, P. Zyla *et al.*, “Review of Particle Physics,” *PTEP* **2020** no. 8, (2020) 083C01.